

Tracking Sunflower Circumnutation using Affine Parametric Active Contours

Suvadip Mukherjee¹, Rituparna Sarkar¹, Joshua Vandenbrink², Scott T. Acton¹ and Benjamin Blackman²

¹Department of Electrical Engineering, University of Virginia

²Department of Biology, University of Virginia

Charlottesville, Virginia, USA

{sm5vp, rs9vj, jpv2n, acton, bkb2f} @virginia.edu

Abstract— Study of the sunflower movement may reveal clues regarding unknown mechanisms that regulate periodicity and spatial complexity in plant growth and development. In this paper, we introduce an automated process to track circumnutation of sunflower seedlings. The objective is to track the leaves of the sunflower plant in a video captured by an overhead camera. The tracking method presented predicts the translated and rotated boundary in the subsequent frames by active contour models. A salient feature of our solution is a constraint on affine transformation between updates. The constrained affine active contours used in this paper exhibit improvement over other traditional active contour approaches, with the new method yielding error less than one percent in the tracked sunflower centroid position.

Keywords— active contours, segmentation, tracking, circumnutation

I. INTRODUCTION

The phenomenon of circumnutation, which is widespread among plants, involves the growth-mediated helical movement of plant organs [1]. These types of movements have been shown to vary in the magnitude (i.e., path length), duration (period of one cycle), shape of the path traced (elliptical, oscillatory along a particular direction or irregular movements along any direction) and direction of rotation (clockwise or counter-clockwise). Also, external stimuli such as light exposure have been shown to influence many aspects of circumnutation behavior. A recently developed population for association mapping in sunflower promises to accelerate the identification of genetic differences among varieties responsible for variation in circumnutation path length, period, shape and direction and thus plant growth [2] [3]. However, the power of such genetic analyses relies on reliably scoring standardized metrics for these spatially and temporally dynamic traits across a large population of hundreds to thousands of individuals. Thus, automated data extraction and quantification of circumnutation characteristics would foster this work and could lead to important discoveries in this aspect of genetic analysis and circadian rhythms.

In this paper we present a method to track the circumnutation of young sunflower plants. The method involves a tracking algorithm based on active contour models to segment the contour of the sunflower plants in successive frames, which undergo a rotational and translational motion along with shape changes. The centroid

locations of the tracked contours can then be exploited to obtain information about the various characteristics of the circumnutation. Due to significant amount of background noise and clutter present in the videos, the traditional parametric active contours [4] tend to be vulnerable to boundary distortion. To reduce the effect of background clutter as well as to efficiently track the rotational-translational motion, the traditional active contour model is constrained by affine transformations. Another advantage of this method is robust estimation of the motion via affine transformation, in contrast to unconstrained movement at each point on the parametric contour. In the following sections, we introduce the tracking framework with a brief summary of traditional active contour techniques, followed by the experimental validation of the theory.

II. ACTIVE CONTOURS FOR TRACKING

Parametric active contours are energy minimizing splines, with a smoothness criterion. The traditional parametric active contour or snake model [4] is defined as a parameterized curve $C(s)$, with parameter $s \in [0,1]$. The curve is realized by iterating on partial differential equations that attempt to minimize an energy functional:

$$E(C(s)) = \frac{1}{2} \int_0^1 \alpha |C'(s)|^2 + \beta |C''(s)|^2 ds + \int_0^1 E_{ext}(C(s)) ds \quad (1)$$

In (1), α and β are weights on the first derivative and second derivative terms in the smoothness constraint. The last term in (1), $E_{ext}(C(s))$, is a data driven energy term, which is minimized at the desired locations, i.e. the object boundaries. A standard practice is to obtain the external energy as $E_{ext}(C(s)) = -|\nabla I(C(s))|$, where $I(\mathbf{x})$ is the 2D grayscale image with domain $\Omega \subset \mathbb{R}^2, \mathbf{x} \in \Omega$. The energy functional can be minimized (locally) using variational calculus, to obtain the following Euler equations for active contour propagation [5]

$$\alpha C''(s) - \beta C''''(s) - \nabla E_{ext}(C(s)) = 0 \quad (2)$$

A numerical solution of the above force balance equation is obtained by using a gradient descent scheme [4]. However, in practice, the standard parametric active contour is sensitive to noise and requires initialization of the contour close to the object boundary. Several methods have been

proposed in the literature to overcome this problem, by introducing a force field with larger capture range to pull the initialized contour towards the desired edges [6] [7] [8].

The above mentioned active contour model can also be used for tracking objects in a video. The active contour model is extensively used for tracking deformable shapes, where the tracked boundary at a frame serves as the initialized contour to segment the object in following frame [9]. The tracking efficiency depends on the presence of noise and clutter, which may force the contour to converge at undesired local minima. Whereas the traditional active contour formulation (1) does not explicitly specify any shape constraints apart from the smoothing parameters, shape priors are often necessary to track objects with known shapes [9], especially in presence of significant clutter.

In this paper, we use parametric active contours to track the motion of sunflower plants. The images are obtained in an indoor growth chamber environment, and reflection from the heterogeneous soil substrate and other plants, for example, pose challenges for designing the tracker (Figure 1). Since it is difficult to model the shape of the sunflowers, we perform tracking by only allowing affine motion of the active contour. The assumption that the motion of the circumnating sunflowers is affine is justified as the videos are captured using overhead camera. In such a perspective, motion exhibited by the flowers is primarily rotational and translational. In the next section, we introduce our technique for tracking using affine active contours [10].

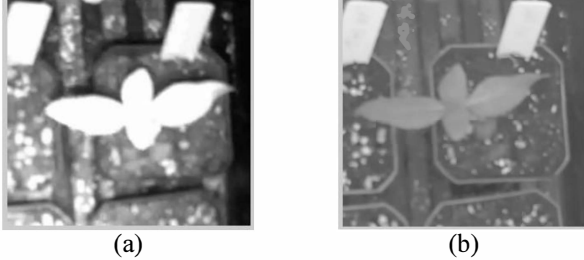


Figure 1 Top view of the sunflower plant under varying illumination conditions. (a) and (b) shows the night time and day time view of the plant respectively and the background clutter present in the video frames.

III. TRACKING WITH AFFINE ACTIVE CONTOURS

Our objective is to analyze the circumnating behavior of the sunflower. This can be performed by tracking the contour of the flower over the successive video frames. The time-lapse videos of the circumnating plants are obtained by capturing images every five minutes over the course of a two-day period (Figure 1). Reflection from the background objects like pebbles, stones and other leaves poses challenge to conventional active contour trackers, thus requiring an approach based on prior knowledge of the shape of the object. Since it is observed that the plants primarily undergo a rotation-translational motion, instead of assigning a shape model, we constrain the evolution of the contour to undergo an affine transformation. The 2D affine transformation of a

parametric contour $C(s) = [X(s) \ Y(s)]$ to a position $C'(s) = [X'(s) \ Y'(s)]$ is given as

$$\begin{bmatrix} X'(s) \\ Y'(s) \end{bmatrix} = \begin{bmatrix} a_1 & b_1 \\ a_2 & b_2 \end{bmatrix} \begin{bmatrix} X(s) \\ Y(s) \end{bmatrix} + \begin{bmatrix} c_1 \\ c_2 \end{bmatrix} \quad (3)$$

The matrix $\begin{bmatrix} a_1 & b_1 \\ a_2 & b_2 \end{bmatrix}$ controls the rotation, scaling and shear for the points on the normalized contour $C(s)$, $s \in [0,1]$ [5], [10]. Translation of the contour points along x and y directions is governed by c_1 and c_2 respectively. These six parameters govern the affine transformation of the 2D curve. Unlike the traditional active contour models where each point on the contour contributes to its evolution, affine active contours can evolve by only modifying the six above mentioned parameters.

A. Affine Active Contour Evolution

As mentioned earlier, 2D affine active contour motion is controlled by the six parameters $\{a_i, b_i, c_i\}_{i=1,2}$. The contour energy functional can be re formulated as

$$E_{affine}(X(s), Y(s)) = \int_0^1 \zeta(X(s), Y(s)) ds \quad (4)$$

Where $C(s) = [X(s) \ Y(s)]'$ is the parameterized curve. $\zeta(\cdot)$ is an image based external energy term that attracts the evolving contour towards the boundary of the object of interest. Minimizing (4) translates to finding the optimal set of parameters which would minimize the external energy $\zeta(\cdot)$ by evolving the curve $C(s)$ through an affine transformation of an initial curve $C_0(s)$. The minimization is performed by taking derivative of the affine energy functional with respect to the parameters $\{a_i, b_i, c_i\}_{i=1,2}$. Mathematically, the energy minimizing curve $C^*(s)$ can be written as

$$C^*(s) = \underset{\{a_i, b_i, c_i\}}{\operatorname{argmin}} E_{affine}(X(s), Y(s)) + \lambda E_{reg} \quad (5)$$

E_{reg} is a term that constrains the affine parameters from changing suddenly. This regularizer is often chosen as $E_{reg} = (a_1 b_2 - a_2 b_1)^2$. λ is a scalar which controls the contribution of the regularizer on the total energy [5].

B. Tracking using Affine Active Contours

Let $C_p(s) = [X_p(s) \ Y_p(s)]'$ denote the detected object boundary at frame 'p'. By allowing affine deformation of the curve, the energy functional at the $(p+1)^{th}$ frame can be written as

$$\begin{aligned} E_{affine}^{p+1}(X_{p+1}(s), Y_{p+1}(s)) \\ = \int_0^1 \zeta(a_1 X_p(s) + b_1 Y_p(s) + c_1, a_2 X_p(s) + b_2 Y_p(s) + c_2) ds \\ + \lambda (a_1 b_2 - a_2 b_1)^2 \end{aligned} \quad (6)$$

Equating the derivative of (6) with respect to $\{a_i, b_i, c_i\}_{i=1,2}$ to zero, we compute the optimal affine

parameters using gradient descent algorithm. This is illustrated in (7).

$$\begin{aligned}
\frac{\partial a_1}{\partial t} &= - \int \zeta_x (X_{p+1}(s), Y_{p+1}(s)) X_p - 2\lambda b_2 (a_1 b_2 - a_2 b_1) \\
\frac{\partial a_2}{\partial t} &= - \int \zeta_y (X_{p+1}(s), Y_{p+1}(s)) X_p + 2\lambda b_1 (a_1 b_2 - a_2 b_1) \\
\frac{\partial b_1}{\partial t} &= - \int \zeta_x (X_{p+1}(s), Y_{p+1}(s)) Y_p + 2\lambda a_2 (a_1 b_2 - a_2 b_1) \\
\frac{\partial b_2}{\partial t} &= - \int \zeta_y (X_{p+1}(s), Y_{p+1}(s)) Y_p - 2\lambda a_1 (a_1 b_2 - a_2 b_1) \\
\frac{\partial c_1}{\partial t} &= - \int \zeta_x (X_{p+1}(s), Y_{p+1}(s)) \\
\frac{\partial c_2}{\partial t} &= - \int \zeta_y (X_{p+1}(s), Y_{p+1}(s))
\end{aligned} \quad (7)$$

Here, t is the pseudo-time for the iterative minimization scheme using gradient descent. By this formulation, the contour can only undergo affine transformation governed by (3). The curve is attracted towards the object edges by the image dependent external force field $\begin{pmatrix} -\zeta_x \\ -\zeta_y \end{pmatrix} = -\nabla \zeta(x, y)$.

We compute this external force using vector field convolution (VFC) [6] on the edge maps of the video frames. This enables the active contour to be attracted towards the target, even if the initial location is not close to the boundary.

IV. EXPERIMENTAL RESULTS

Initial experiments were performed on videos of sunflowers, where the plants were subject to varying illumination conditions. The initial contour was obtained by manually tracing the boundary of the plant using the Livewire segmentation technique [11]. The affine active contour tracker was used to automatically segment the plant boundaries in the subsequent frames. The parameters of the affine contour model were initialized as $a_1 = 1, b_1 = 0, a_2 = 1, b_2 = 0, c_1 = 0, c_2 = 0$. Parameter update is performed sequentially by implementing (7) on a discrete grid till a convergence criterion is satisfied. Sample tracking results are shown in Figure 4. The proposed method is compared to the traditional active contour tracker with vector field convolution (VFC) external force [6, 1]. It is observed from the comparison results that the affine active contour model is more robust to background clutter whereas the traditional active contour is sensitive to noise and background changes.

The normalized mean squared error between the tracked centroid and the manually obtained plant center is plotted for 50 consecutive frames. Figure 2 shows the normalized mean squared error graph for two videos and is compared with VFC-based active contour. For both videos, affine active contours result in less than 1% error.

The spatial position of the sunflower centroid with time is shown in Figure 3. The plant motion occurs in a helical pattern comprising of a circular motion along with its growth in height. Hence, we expect a periodic motion pattern of the tracked centroid with respect to time, which is

observed in the 3D plot in Figure 3. From the centroid location in the graph, information about the different circumnutation characteristics, i.e., the path length, duration of one cycle, shape of the path and rotational direction, can be computed.

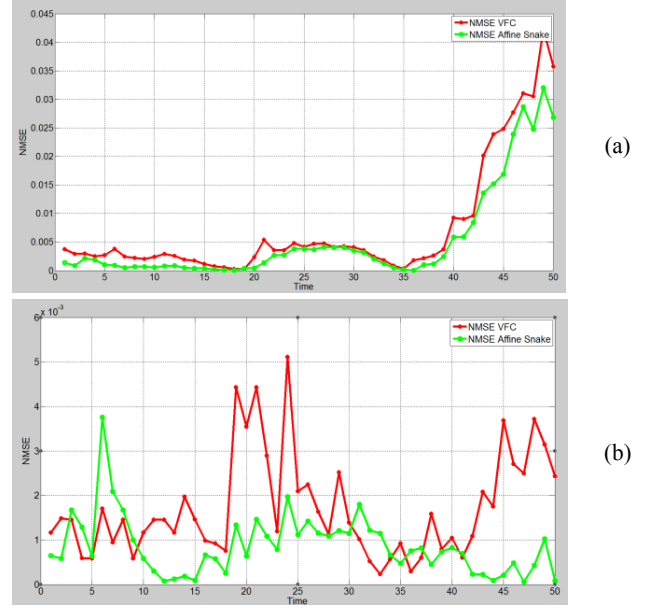


Figure 2: The normalized mean squared error for video 1 and 2 are shown in (a) and (b) respectively. Affine AC results are in green and the VFC based technique is plotted in red.

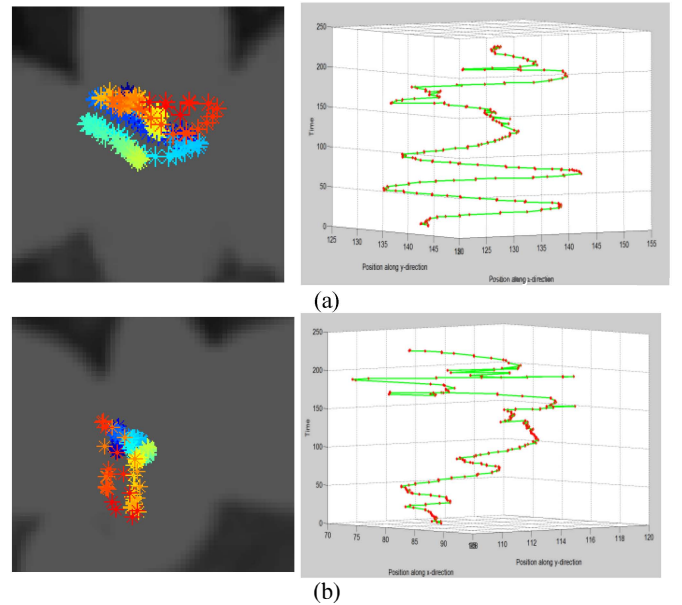


Figure 3: (a) and (b) show the spatial position plots of the sunflower with respect to time. The left column gives the spatial position on the observed region with time, and the color changes from blue to red with time. The right column gives the 3D plot for the position in space with time.

V. CONCLUSION

In this paper, we have introduced a scheme to track the circumnutation of the sunflower plant. Affine active contour models provide an efficient and robust way of tracking the motion of the plant in presence of significant background clutter, which is supported by the preliminary experimental results. However, the performance of the tracker degrades in cases where the background illumination changes abruptly. Since a majority of the videos are obtained in diurnal environment, we wish to introduce a method to model the illumination variation in our future work.

REFERENCES

- [1] S. Mancuso and S. Shabala, *Rhythms in Plants: Phenomenology, Mechanisms, and Adaptive Significance*, Berlin: Springer, 2007.
- [2] J. Mandel, et al., "Genetic diversity and population structure in cultivated sunflower and a comparison to its wild progenitor, *Helianthus annuus* L.," *Theoretical and Applied Genetics*, vol. 123(5), pp. 693-704, 2011.
- [3] J. Mandel, et al., "Association Mapping and the Genomic Consequences of Selection in Sunflower," *PLoS Genetics*, vol. 9(3), e1003378, 2013.
- [4] M. Kass, A. Witkin and D. Terzopoulos, "Snakes: Active COntour Models," *IJCV*, 1988.
- [5] S. T. Acton and N. Ray, *Biomedical Image Analysis*, Morgan & Claypool Publishers, 2006.
- [6] B. Li and S.T. Acton, "Active contour external force using vector field convolution for image segmentation," *IEEE, Trans. on Image Procs.*, vol. 16, pp. 2096-2106, 2007.
- [7] C. Yang and S. T. Acton, "External forces for active contours via multi-scale vector field convolution," in *IEEE International Conference on Image Processing*, 2012.
- [8] C. Xu and J. L. Prince, "Snakes, shapes, and gradient vector flow," *IEEE Transactions on Image Processing*, vol. 7.3, pp. 359-369, 1998.
- [9] N. Ray, S. T. Acton and K. Ley, "Tracking leukocytes in vivo with shape and size constrained active contours," *IEEE Trans. on Medical Imaging*, vol. 21.10, pp. 1222-1235, 2002.
- [10] D. P. Mukherjee and S. T. Acton, "Affine and projective active contour models," *Pattern recognition*, vol. 40.3, pp. 920-930, 2007.
- [11] E. N. Mortensen and W. A. Barrett, "Intelligent scissors for image composition," in *ACM Proceedings of the 22nd annual conference on Computer graphics and interactive techniques*, 1995.

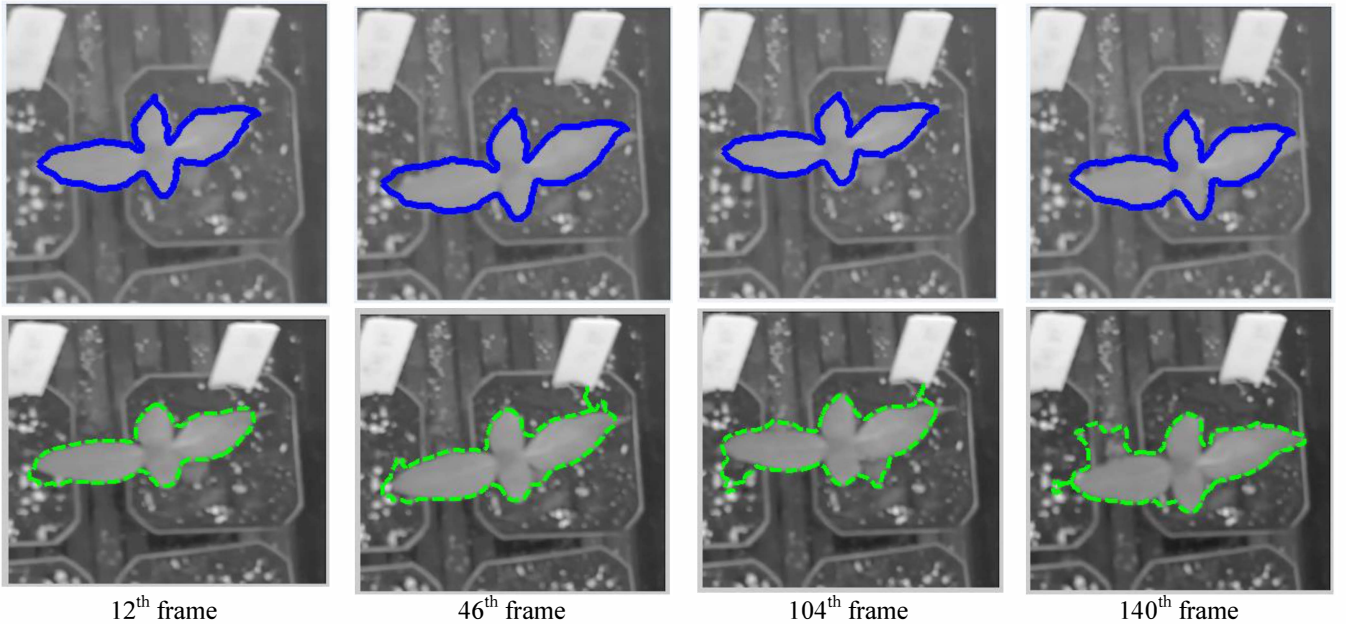


Figure 4: Comparison of affine active contours (in blue) and VFC based active contour without shape prior (in green).